

Article

# Tool for Quantitative Risk Analysis of Urban Flooding

Julia Kvitsjøen <sup>1,2,\*</sup> , Dick Karlsson <sup>3</sup>, Trym Teigene <sup>4</sup> and Webjørn Finsland <sup>4</sup>

<sup>1</sup> Faculty of Science and Technology, Norwegian University of Life Sciences, 1430 Ås, Norway

<sup>2</sup> The Agency for Water and Wastewater Services, City of Oslo, Herslebs Gate 5, 0561 Oslo, Norway

<sup>3</sup> Sustainable Waste and Water, City of Gothenburg, Gamlestadsvägen 317, 42423 Angered, Sweden; dick.karlsson@kretsloppochvatten.goteborg.se

<sup>4</sup> The Agency for Planning and Building Services, City of Oslo, Vahls Gate 1, 0187 Oslo, Norway; trym.teigene@pbe.oslo.kommune.no (T.T.); webjorn.finsland@pbe.oslo.kommune.no (W.F.)

\* Correspondence: julia.kvitsjoen@vav.oslo.kommune.no

**Abstract:** One of the effects of climate change is an increasing frequency of heavy rainfall events, which in turn leads to increased flooding damage in urban areas. The purpose of this study was to develop a tool for dynamic risk evaluation that can be used to fulfil several of the goals in the European Flood Risk Management Directive. Flood risk analysis was performed as a spatial GIS analysis with the FME software. The primary data source for the analysis was a 1D/2D model calculation, wherein 1D models described the pipeline network and the watercourses and a 2D model described surface runoff. An ArcGIS online platform was developed to visualize the results in a format understandable for decision makers. The method and tool were tested for the Norwegian capital of Oslo. The tool developed in the study enabled the efficient analysis of consequences for various precipitation scenarios. Results could be used to identify the areas most vulnerable to flooding and prioritize areas in which measures need to be implemented. The study showed that for urban areas in steep terrain, it is essential to include water velocity and depth-integrated velocity in risk analysis in addition to water depths and pipe network capacity.

**Keywords:** climate change adaptation; cloud burst management; quantitative risk analysis; urban flooding; urbanization



**Citation:** Kvitsjøen, J.; Karlsson, D.; Teigene, T.; Finsland, W. Tool for Quantitative Risk Analysis of Urban Flooding. *Water* **2021**, *13*, 2771. <https://doi.org/10.3390/w13192771>

Academic Editor: Martina Zelenakova

Received: 18 August 2021

Accepted: 1 October 2021

Published: 6 October 2021

**Publisher's Note:** MDPI stays neutral with regard to jurisdictional claims in published maps and institutional affiliations.



**Copyright:** © 2021 by the authors. Licensee MDPI, Basel, Switzerland. This article is an open access article distributed under the terms and conditions of the Creative Commons Attribution (CC BY) license (<https://creativecommons.org/licenses/by/4.0/>).

## 1. Introduction

Flood is defined as “the temporary covering by water of land not normally covered by water” in the European Flood Risk Management Directive (Flood Directive) [1] (p. 3). Many cities worldwide have reported increasing damage from floods [2–8], including urban flooding; “urban flooding is the accumulation of floodwaters that result when the inflow of storm water exceeds the capacity of a drainage system to infiltrate water into the soil or to carry it away” [9] (p. 9). Urban flooding can occur from several sources depending on the location of the urban environment: pluvial floods, fluvial floods, storm surges, or high tides in coastal areas.

More intensive and frequent extreme rainfall events with associated floods have been projected for Europe with medium to high confidence [10]. There is also high confidence that the combination of sea-level rise, storm surges in coastal cities, and extreme rainfall/river flow events will make flooding more probable. Although the climate is getting wetter in several parts of the world, climate change alone does not always increase flooding damage. Another significant factor is urban densification. Urbanization increases mean and heavy precipitation over cities, thus resulting in higher runoff intensity [10]. There are also many other factors in a city affecting runoff: (a) it increasingly rains more than drainage systems are designed for, and the capacity of drainage systems has deteriorated over time; (b) natural runoff routes are blocked by infrastructure; and (c) large parts of urban areas have become impermeable.

Although there is uncertainty regarding future rainfall patterns, it is highly probable that intensive rainfall will occur more frequently, and flooding damage will increase if risk-reducing measures are not integrated into urban development. Adapting cities to climate change is a complex and long-term process. Nevertheless, because of the expected damage costs, rapid and effective action is needed now [11]. Adaptation measures must be based on robust data and risk assessment tools. Risk analysis of urban flooding is essential for securing inhabitants and infrastructure in urban areas that are most vulnerable to flooding. Knowing the extent, probability, and location of potential problems will enable public decision makers to prioritize emergency preparedness and prevention measures.

In the Flood Directive, flood risk is defined as “the combination of the probability of flood event and the potential adverse consequences for human health, the environment, cultural heritage, and economic activity associated with a flood event” [1] (p. 3). Like other European Union countries, Sweden has implemented the Flood Directive in national guidelines for risk analysis [12]. The Norwegian Water Resources and Energy Directorate has also followed up the Flood Directive in the national framework for assessing and managing flood risks [13]. The assessment and management of pluvial floods in urban environments are not directly covered by the Flood Directive, but are implemented at the national level in several countries. For instance, guidance materials for conducting urban flood risk analyses have been prepared in Norway [14] and Sweden [15]. Methodological approaches and levels of detail for such risk analyses vary between different cities. Traditionally, a qualitative method is used for flood risk analysis [14,16,17]. Qualitative risk analysis determines severity of flooding by presenting results in a risk assessment matrix. The method is particularly useful when there is insufficient knowledge of probabilities [16]. Quantitative risk analysis uses verifiable data to analyse the consequences of different risks [15,17–20].

Qualitative identification of risks based on professional and local knowledge is widespread. Qualitative flood risk analysis does not require any digital tools and is more accessible to public administrations than the quantitative method. The challenge is that qualitative assessment mainly uses a rather coarse hazard classification and is limited to representing the flood risk [17]. The method is also subjective. It is especially challenging to produce a reliable analysis for large cities, locate risks geographically, and identify the extent of damage for different rainfall scenarios. Several cities and towns in the Nordic countries have experienced severe urban flooding in recent years [2–4,8]. Nevertheless, assessments of the potential damage of extreme precipitation in urban areas that so far have not experienced such events are often based on the lessons learned from “famous” flooding events in neighbouring countries. For instance, the 2011 flood in Copenhagen, Denmark, is used as a template for the qualitative assessment of potential damage in Norway, albeit with some adjustment to local conditions [18,19].

As an intermediate stage between qualitative and quantitative risk analysis, GIS terrain [13] and historical loss data analyses [9] can be used. These tools allow better visualization of risks than studies based purely on experience. Furthermore, GIS analysis provides the opportunity to include water depth as a damage parameter. However, the information from GIS analysis may be incorrect because several parameters, such as pipe network capacity, infiltration, hydrodynamics, and the time-space distribution of precipitation runoff, are not included. Furthermore, water depth is not always correlated with the extent of damage, especially in urban areas with steep terrain.

Quantitative analysis can be performed based on the results from hydraulic modelling [9]. A risk analysis based on 2D hydraulic models of surface runoff includes both hydrological and hydraulic parameters, requires a limited amount of input data, and provides a quick overview of flooding at extreme precipitation events. Decision makers can choose 2D models for the assessment of flood risk for critical infrastructure [20]. However, one of the most significant uncertainties in the 2D hydraulic model is the omission of pipeline network capacity and potential flow exchange with watercourses. These two factors may be necessary to assess several risk categories in addition to risk to critical infrastructure.

The modelling must be sufficiently detailed and flexible to properly represent the flow pathways, the full extent of the flooding, and the watercourse's hydraulics [21]. One- and two-dimensional coupled models can give a broad description of complex urban hydrology as input data to the risk assessment of urban flooding. Several studies have developed models for flood simulation by coupling 1D models for watercourses with 2D overland flow [21–24]. In a Norwegian study, a large-scale full hydrodynamic model was developed for Oslo [25]. The model enabled water flow analysis on the surface, in the drainage pipe network, and in watercourses. Nine 1D models for main rivers in Oslo were coupled by lateral links to ten 2D flexible mesh (FM) surface runoff models (1D/2D coupling). The 1D model for the pipeline network (44,000 pipes with associated installations) was coupled by outlets to 1D river models (1D/1D coupling) and by manholes to eleven 2D FM models with a total area of 185 km<sup>2</sup> (1D/2D coupling). Despite its great complexity, scope, and level of detail, the model had high computational efficiency. This was achieved by using flexible mesh for the 2D models and a GPU processor for calculations [21,25].

The EU Strategy on Adaptation to Climate Change highlighted the need to close knowledge gaps on climate impacts and resilience and improve technology in climate adaptation modelling, risk assessment, and management tools [11]. This study was based on the need to cover knowledge gaps in quantitative risk analysis of urban flooding to achieve various objectives in the Flood Directive [1]. The study's primary goal was to develop and test a methodology and tool for the systematization and analysis of hydraulic modelling results for a wide range of risk categories to efficiently analyse the consequences of various precipitation scenarios in large urban areas. The results should provide a basis for identifying problem locations, prioritizing areas for measures, and prioritizing types of actions for different areas within the study area—the Norwegian capital of Oslo. The database in the study was limited to pluvial floods, but results from the assessment will be useful for quantifying the risk of urban flooding regardless of the cause of the flooding.

## 2. Materials and Methods

The method for risk analysis developed and tested in this study was based on hydraulic modelling (Figure 1). Thus, when starting a risk analysis, it was necessary to identify for which precipitation scenario (probability) and for which associated risk categories the consequences are to be assessed [26]. A survey of the municipal map database was made to identify map layers that are available for analysis. Based on this information, risk types for each risk category [14,19] were identified. The definition of damage thresholds for different types of risk was based on a literature study [20,21], with some adaptation to available data and local knowledge. A GIS-based spatial overlay analysis that included and weights all available datasets was set up in the Feature Manipulation Engine (FME) software [27]. All potential risks cannot always be identified quantitatively, and there is still a need for qualitative assessment of specific risk categories [16]. However, because of good data access in this study, quantitative analysis was considered sufficient to obtain a reliable result, and a qualitative follow-up was not included in this study. ArcMap [28] was used to visualize consequences per risk type and per risk category as well as total risk at a given probability. Finally, an online ArcGIS tool [28] was developed to visualize the results for decision makers. The use of results was not a part of this study.

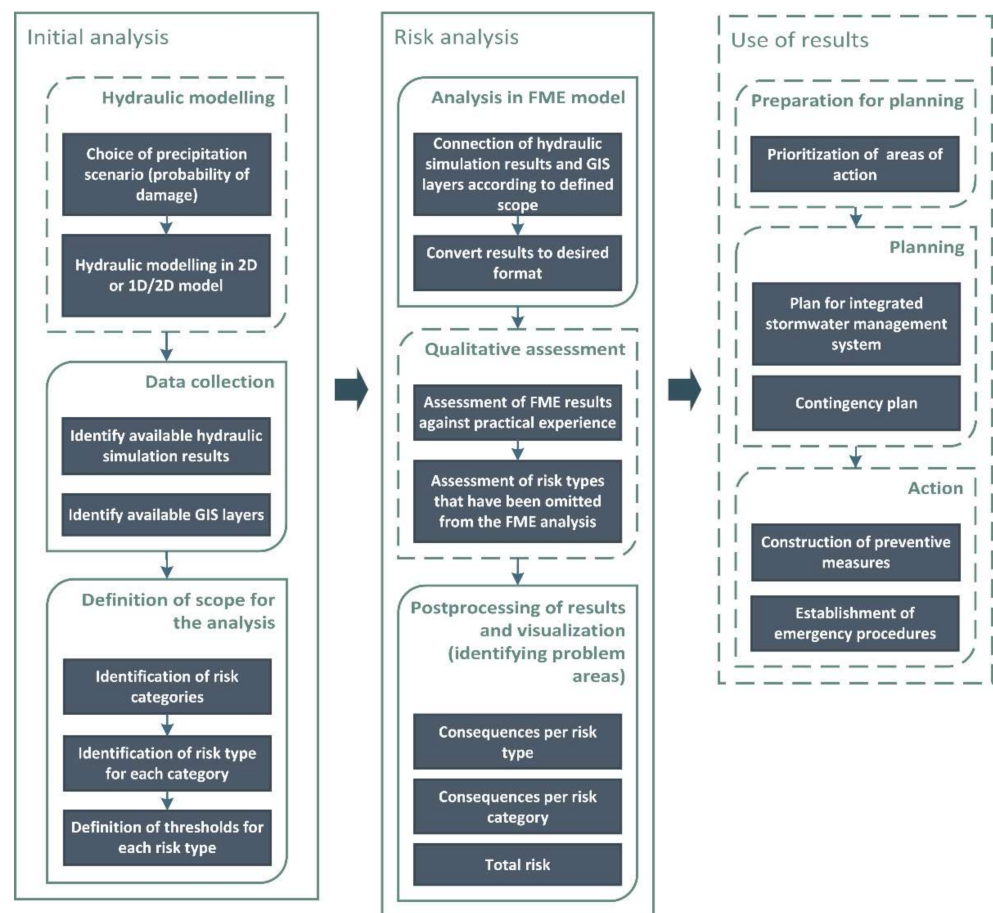


**Figure 1.** Assessments of flood risk for a wide range of risk categories in urban areas using hydraulic and FME models.

### 2.1. Study Area

In this study, the Norwegian capital Oslo was used as the study area. The area of Oslo municipality is 454 km<sup>2</sup>, but the city itself, with 700,000 inhabitants, has an area of 147 km<sup>2</sup>.

Oslo is characterized by significant variations in the terrain. While the downtown area in Oslo is at sea level, the upper edges of the city are at elevations of 200–500 masl. Annual precipitation at the central MET office station is 780 mm [29]. The wastewater network in Oslo has a total length of 2250 km [30]. Approximately 55% of the wastewater network in Oslo is combined sewer system (CS). The network includes 218 combined sewer system overflows (CSOs) that discharge into the city's watercourses and the Oslo Fjord. Historically, there were 353 km of open streams and rivers in the Oslo area. However, 66.8% of stream routes have been piped or buried. Some of them are now part of the drainage and sewer systems, but others are entirely buried. A total of 10 rivers and streams with natural catchments flow through urban parts of Oslo before being discharged into the fjord. The study method and the tool were first tested for one of the main river catchment areas, Akerselva, with a substantial local flood knowledge base before it was implemented for the entire city [9] (Figure 2).

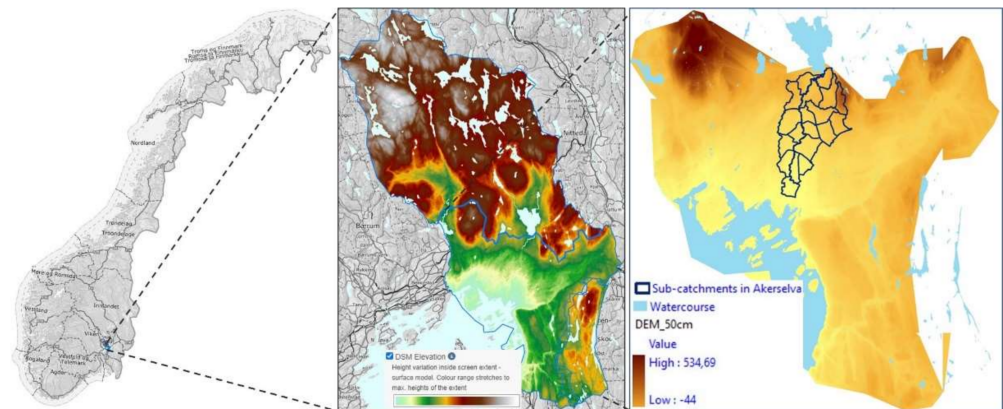


**Figure 2.** Location and elevation for Oslo and Akerselva study areas.

### 2.2. Input Data from Hydraulic Modelling

Prior to this study, DHI Norway (DHI) carried out hydraulic modelling in an uncalibrated 1D/2D MIKE FLOOD model [25] that connects three models: MIKE 21 FM, MIKE HYDRO River, and MIKE URBAN CS [31]. A detailed description of the model construction can be found in the DHI model report [25].

An intensity–duration–frequency curve (IDF) was developed for a future 200-year rainfall event by multiplying IDF for the current 200 return period (50 mm per hour) with a climate factor of 1.5 (200CF), based on statistical precipitation data from the weather station at Blindern, Oslo (1967–2019) [29] and the expected climate factor [32]. The model for the test area of Akerselva was run for 200CF for the development phase of the tool.

To cover the risk of damage to critical infrastructure, the effects of urban flooding on the entire city were calculated for a 1000-year return period [33]. However, there are limited statistics on extreme precipitation events. Although there have been short-term extreme precipitation events in recent years throughout the Nordic countries, these were often poorly documented because of local rains not being captured by measuring stations. Thus, in this study, an actual rainfall event in Copenhagen (155 mm per 2 h) on 2 July 2011 (CPH) was applied [34], since appropriate rainfall data for Oslo were not available [26]. This event is believed to be comparable to a 1000-year rainfall event in Oslo.

### 2.3. Risk Categories Divided into Risk Types

In this study, damage consequences were calculated for six risk categories: human life and health, nature and environment, critical infrastructure, vulnerable societal functions (F3), building damage (F1 and F2), and accessibility. The classification of buildings in F1, F2, and F3 [33] can be found in Table 1.

**Table 1.** Classification of buildings in the risk categories “vulnerable social functions (F3)” and “building damage (F1 or F2)”.

Risk Category	Content
4—Vulnerable social functions (F3)	Hospital, Nursing home, Fire station, Police station, Civil defence facilities, Kindergarten, Train/Metro station, Other shielded objects
5—Building damage (F1 or F2)	All other buildings not covered by F3

The selection of risk categories was partly adapted from the existing categorization of consequences in national guidelines for risk analysis in Norway [14,19]. Each risk category described two to four different risk types based on local knowledge and available data. Risk categories with associated risk types, as well as GIS map layers needed for analysis and modelling results, are summarized in Table 2.

**Table 2.** Risk categories with associated risk types as well as GIS map layers necessary for analysis and modelling results (CS—combined sewer system, D—water depth, V—water velocity, DV—depth-integrated water velocity, P—pressure level in CS, Q—accumulated water volume).

Nr	Risk Category	Risk Type	GIS Map Layer	1D/2D Model Results	Risk Output Unit
1	Human life and health	Drowning and instability of humans	All areas except buildings	D, V, DV	m <sup>2</sup>
		Basement flooding—health risk from pollution in buildings	DEM, CS, branch pipes, buildings, year of construction for buildings	P	Number of buildings
		Accumulation from CS manholes on the surface (ACS)—health risk from pollution outside	All areas except buildings, CS	Q	Number of manholes
		Combined sewage overflow (CSO)—health risk when bathing	Watercourses, CS	Q	Number of CSOs
2	Nature and environment	Flooding	Cultural heritage and protected objects, petrol stations, companies with chemical production, landfills	D	Number of cultural heritages etc.
		Erosion	On discontinued landfills	D, V	m <sup>2</sup>
		CSO	Watercourses, CS	Q	Number of CSOs
		ACS—pollution in urban spaces	Green areas, CS	Q	Number of manholes
3	Critical infrastructure	Flooding	Electrical transformers, pumping stations	D	Number of TS/PS
		Erosion	On the ditch routes, road/green areas	D, V	m <sup>2</sup>
4	Vulnerable social functions (F3)	Flooding	Building class F3	D	Number of F3
		Basement flooding	DEM, CS, branch pipes, buildings, year of construction for buildings	P	Number of F3
		Erosion	At building class F3	D, V	Number of F3
5	Building damage (F1 and F2)	Flooding	Building class F1 or F2	D	Number of F1–F2
		Basement flooding	DEM, CS, branch pipes, buildings, year of construction for buildings	P	Number of F1–F2
		Erosion	At building class F1 or F2	D, V	Number of F1–F2
6	Accessibility	Traffic jams (6.1, 6.2, or 6.3) and instability of vehicles (6.1 or 6.2)	Road (6.1), emergency routes (6.2) subway/train (6.3)	DV, D	m <sup>2</sup>
		Erosion	Road (6.1), subway/train (6.3)	D, V	m <sup>2</sup>

For the first risk category, “human life and health”, four types of risk were identified. Humans can be exposed to harm at great water depths (D). In areas with steep terrain, injuries can also occur at low D but with high water velocity (V). The risk of human instability in water flow, friction stability (sliding), and moment stability (rolling) can be described at depth-integrated water velocity. In this study, only an assessment of moment stability (DV) was included in the analysis. Assessments of D, V, and DV were performed for all areas in the city except buildings.

As well as by mechanical influences, people can be exposed to harm by contamination from a sewer [35]. Three analyses identified the risk of sewer pollution: basement flooding, accumulation from manholes on surface (ACS), and overflows to watercourses (CSOs) from the combined sewer system (CS). The study included only the risk of pollution, but not of the concentration of pollutants, because of the lack of data for pollutant concentration from modelling.

The basement flooding risk was identified by connecting results for pressure level (P) in CS to associated buildings via branch pipes in the FME model. In the overall analysis

for an entire city, it was too time-consuming to analyse the exact depth of pipelines and building basements relative to each other. Basement data registered by the municipality were also uncertain. Therefore, a simplification was made. The digital terrain model was used to calculate altitude variations between the start and stop points on branch lines. Public requirements for a minimum height of the basement hatch level in Oslo were changed in 1982 [36]. Therefore, information about the construction year was included in the analysis. Health risks from polluted water at ACS and CSO were identified by assessing the accumulated water volume (Q) on the terrain and from CSO.

For the risk category “nature and environment”, four risk types were analysed: flooding, erosion, CSO, and ACS. Water depth (D) was used to analyse flooding of infrastructure that may adversely affect the environment. Such infrastructure included, for example, landfills and companies that handle environmentally hazardous chemicals. In addition to the aspect of environmental pollution, the risk category includes flooding of objects with cultural and historical value. Decommissioned landfills are covered and are not affected by flooding, but they can nevertheless pose an environmental risk in the case of erosion. Although the assessment of CSO and ACS was included in analysing health risk in the first risk category, these two parameters also negatively affect the environment.

Analysis of the risk of damage in critical infrastructure consisted of an assessment of two types of risk. Flooding of electrical transformers and pumping stations can have a significant impact on a city’s functionality. As the risk of erosion varies depending on the grain size of the surface substrate, the calculation of erosion was performed separately for permeable and impermeable surfaces. Large parts of the underground infrastructure, in the form of cables and pipes, are located along the ditch routes of water and wastewater pipes. By buffering a GIS layer for the pipe network with one metre on each side, ditch width was estimated in a new map layer for ditch routes.

For the risk categories “vulnerable social functions (F3)” and “building damage (F1 and F2)”, three risk types were analysed: flooding, basement flooding, and the risk of landslides due to erosion, as described above. The building classification was based on regulations [33], with minor adjustments to local conditions (Table 1).

The assessment of “accessibility” was divided into three separate assessments: all roads, roads used as emergency routes, and subway/train tracks (6.1, 6.2, and 6.3; Table 2). Deep water can lead to traffic jams, while depth-integrated water velocity can affect vehicle stability. Erosion risk was assessed for all roads and subway/train tracks.

#### 2.4. FME Model

The impact assessment was carried out in the FME model [27] by connecting the GIS map layers and simulation results from the 1D/2D coupled hydraulic model with associated thresholds. GIS map layers were obtained from the map database of the City of Oslo. Model simulation results were converted to raster with a resolution of 1 m×1 m. Maximum values for D (supplementary materials) and V were obtained from raster model results for each cell. Accumulated water flow (Q) from manholes on the terrain and from CSOs were obtained using MIKE View [31]. Maximum values for DV were identified by multiplying D and V for each cell for each calculation step in MIKE Zero [31]. Pressure in CS (P) was postcalculated in MIKE URBAN CS [31] based on simulation results. Inspired by literature [20,21,31], the threshold values in the present study were complemented by practical experience and linked to the associated risk types in the FME model, as shown in Table 3.

Three risk classes were chosen as a starting point: low, medium, and high. However, considering further application of the FME model in more detailed studies, consequences were calculated for five risk classes for those risk types for which it was possible to identify suitable risk thresholds.

Classification of drowning and instability of humans in water flow was performed by assessing D, V, and DV.

**Table 3.** Basis for setting up the FME model for impact assessment with risk types and associated thresholds for damage distributed among associated risk classes. Adapted from [20,21,31]. (RC—risk category, CSO—combined sewer overflow, ACS—accumulation from manholes on surface. Units: D (m), V (m/s), DV (m<sup>2</sup>/s), P (m), Q (l/s), O (m).)

Risk Type	Low		Medium		High
	1	2	3	4	5
Drowning and instability of humans, RC 1	DV = 0.1–0.4 or D = 0.1–0.2	DV = 0.4–0.6 or D = 0.2–0.3	DV = 0.6–0.8 or D = 0.3–0.4	DV = 0.8–1.2 or D = 0.4–1.2	DV > 1.2 or D > 1.2 or V > 3
Flooding, RC 2, 3, 4, 5	D > 0.2 0–12% O	D > 0.2 13–25% O	D > 0.2 26–38% O	D > 0.2 39–50% O	D > 0.2 >50% O
Flooding, RC 3	D > 0.2 for <2 TS/PS		D > 0.2 for 2–10 TS/PS		D > 0.2 for >10 TS/PS
Traffic jam, RC 6.1	DV < 0.3 and D < 0.1	DV < 0.3 and D < 0.2	DV = 0.3–0.6 and D < 0.2	DV < 0.6 and D = 0.2–0.5	DV > 0.6 and D > 0.5
Traffic jam, RC 6.2	DV < 0.3 and D < 0.1		DV = 0.3–0.6 and D < 0.2		DV > 0.6 and D > 0.2
Traffic jam, RC 6.3	D > 0.05		D > 0.1		D > 0.3
Erosion, RC 2, 3, 4, 5, 6	Loose cover and D > 0.1 and V > 0.5		Loose cover and D > 0.1 or V > 1		Loose cover and D > 0.1 and V = 2
	Hardcover and D > 0.1 and V > 2		Hardcover or D > 0.1 and V > 3		Hardcover and D > 0.1 and V > 4
Basement flooding, RC 1, 5	P > 0.9 for buildings constructed after 1982 and P > 0.5 for the rest				
CSO, RC 1, 2	Q < 5		5 < Q < 100		Q > 100
ACS, RC 1, 2	Q < 5		5 < Q < 100		Q > 100

Some risk types described in Table 2 were repetitive for different risk categories (RC). For example, the risk type “Flooding” affects buildings under RC 2, 3, 4, and 5 (Table 3). The analysis was therefore run collectively for all buildings (Figure 3).

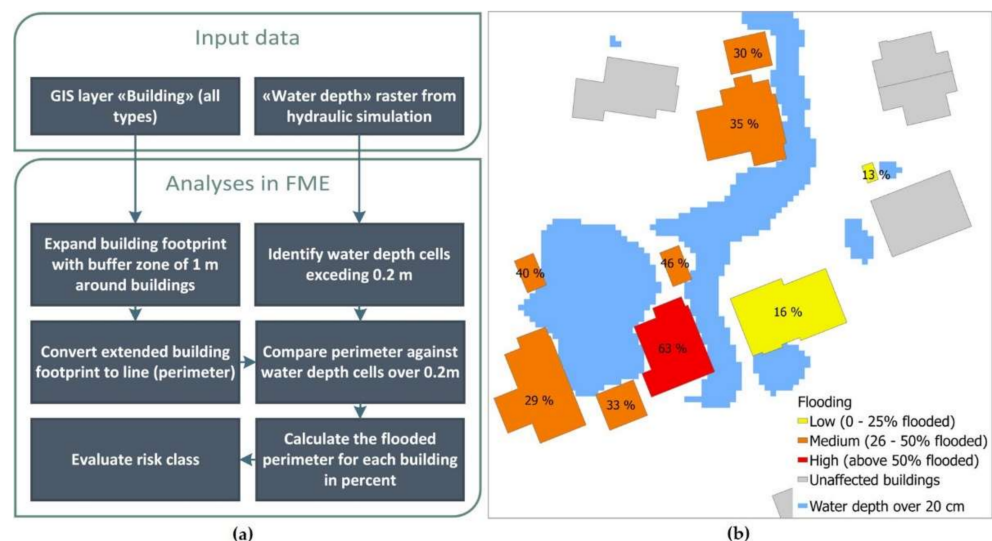


**Figure 3.** Flow chart for calculation process in FME (a); percentages of building perimeters flooded with associated risk classes (b).

The analysis assumed that buildings could be damaged by flooding at water depths greater than 0.2 m. The extent of damage depended on the number of water-filled GIS cells adjacent to the perimeter (O) of the building. Because of some minor inaccuracies in the description of buildings in the MIKE 21 model, water-filled cells from modelling

results did not necessarily affect the building's perimeter. Therefore, a buffer zone of one metre was created around buildings. After converting the extended polygon of building footprints to the perimeter, the perimeter was compared against water depth cells over 0.2 m. The tool calculated flooding percent and evaluated risk class. Associated building properties were retained to identify buildings for each RC after the impact assessment.

Electrical transformers and pumping stations (TS/PS) were counted per geographical distributed area of interest to generalize the risk for critical objects when presenting results.

A general assessment of accessibility on all roads was conducted with thresholds for D and DV for RC = 6.1. As emergency routes are of great importance in a critical flooding situation, stricter thresholds were set for impact testing. In other studies [37], the risk of delaying emergency vehicles was assessed with fewer rigour thresholds because, for example, a fire truck can drive through deeper water and withstand higher water flow than passenger vehicles. Nevertheless, in a dense city, the accessibility of even heavy emergency vehicles is affected by other traffic on the road. Even smaller flooded areas along train and metro tracks can cause traffic jams because electrical control units can go out of service.

Erosion was another parameter that was included in the assessment of several risk categories. The risk of erosion was examined for loose cover and hardcover for the entire city when assessing D and V.

The connection of the 2D surface model and the 1D pipe network model via man-holes provided an imprecise description of water exchange between the surface and pipe network in an uncalibrated model. Calculating the risk of ACS reduces uncertainty for building damage from surface flooding. When assessing the risk of basement flooding, two thresholds were used based on regulatory changes. For buildings built before 1982, basement flooding could occur at a pressure level of 0.5 m above the top pipe. For newer buildings, the risk was reduced to a pressure level of 0.9 m. Only buildings connected to CS were considered in this analysis.

Pollution risk from ACS and CSO was assessed as the amount of wastewater from the CS. In the study, no priority was given to calculating pollutant concentration from CS. Values for different types of risk were based on practical experience.

### 2.5. Result Summary

The overall risk for each risk category and total risk were calculated for different geographical units. Three types of geographical area distribution were analysed: main river catchments, subcatchments in the Akerselva catchment, and administrative districts in Oslo.

The calculation was performed in the FME model. At the first, the consequences for all risk types (RT) within a risk category (RC) were summarized for each cell on the map per geographically distributed area of interest (GA) (1). The cell size used in this study was 1 m<sup>2</sup>.

$$\text{Consequence } RC(x)_{GA} = \frac{\sum_{i=1}^n \text{Consequence } RT(x)_{cell}}{\text{Area}_{GA}} \quad (1)$$

The relative consequence distribution (RCD) for each risk category was calculated with the help of Formula (2). The GA with the most significant consequence was assigned a score of 100%. Consequences were distributed to the remaining GAs, relative to the GA field with the highest consequence, to weigh consequences for each risk category among GAs.

$$\text{Relative consequence distribution } RC (RCD) = \frac{\text{Consequence } RC_{GA, x}}{\text{Consequence } RC_{GA, max}} \times 100\% \quad (2)$$

Total risk was identified by an overall assessment of all risk categories for each GA (3).

$$\text{Total risk} = \frac{RCD_1 + RCD_2 + RCD_3 + RCD_4 + RCD_5 + RCD_6}{6} \quad (3)$$

The significance of risk types for each risk category and the significance of each risk category for the total risk were weighted equally in this study, but could be weighted differently based on local preferences.

## 2.6. Visualization of Results

Visualization of results depends on the user group (Figure 4) [9,38]. Results from this study would be used internally in the city of Oslo in the first instance. It was thus a priority to focus on visualization level 1 for public planning and emergency preparedness.

		Visualization level 1	Visualization level 2	Visualization level 3
Target group-oriented information about flood risk	Objective	Consideration in planning and operation	Private prevention, property protection	Transfer of risk information
	Target group	<b>Public:</b> City/spatial/traffic planning Municipal sewage company Fire brigade, police, etc.	<b>Private:</b> Property owners Architects Construction companies	<b>Media:</b> Print media Broadcasting, TV Internet, social media

**Figure 4.** Visualization levels by objective and target group for flood risk communication. Adapted from [38].

FME results can be processed and visualized in several ways, depending on the purpose of the visualization. For a municipality, it is crucial to prioritize investment in areas in which the most severe impact of urban flooding can be expected. Analysis of consequences of different risk types is useful for detailed studies and planning of emergency preparedness and preventive measures. For example, erosion risk can be described as a separate map layer with respective risk colours, regardless of which risk category said colours are linked to. Consequences of erosion per risk type can be visualized according to the risk types in Table 3. Another option would be to survey how each risk type is affected by erosion, for example, building type or area types such as roads or parks.

To establish a prioritization basis for further action planning, overall risk categories and total risk for different areas in the city can be presented as polygons with associated colours for three risk classes.

Visualization of results in this study was performed both in ArcMap [28] and with predefined functionality in ArcGIS online [28]. The colour palette from Table 3 was used for all result presentations. When visualizing the consequences for risk categories and total risk, calculated risk values were distributed using “natural breaks”. Results from the FME calculation were retrieved into ArcGIS online and relevant map layers, for example, the background map. The visual presentation of results and colour formatting were adjusted as desired. Access was differentiated to different user groups based on service needs.

## 3. Results

### 3.1. Consequences per Risk Type

Consequences per risk type were calculated and visualized according to the risk types in Table 3, making it possible to assess the risk for each object in the city separately. Results showed a clear distribution of the potential risk of drowning and instability for humans in various open areas within the test area, Akerselva, at the 200-year incident with climate factor (200CF). Similarly, it was possible to see which roads and subway/train tracks could be expected to experience traffic jams. Several buildings of different categories were exposed to different levels of damage risk from flooding, basement flooding, erosion, or a combination of different types of risk. The method also allowed the classification of discharge risk from CSOs and CS manholes based on model simulations (Figure 5).

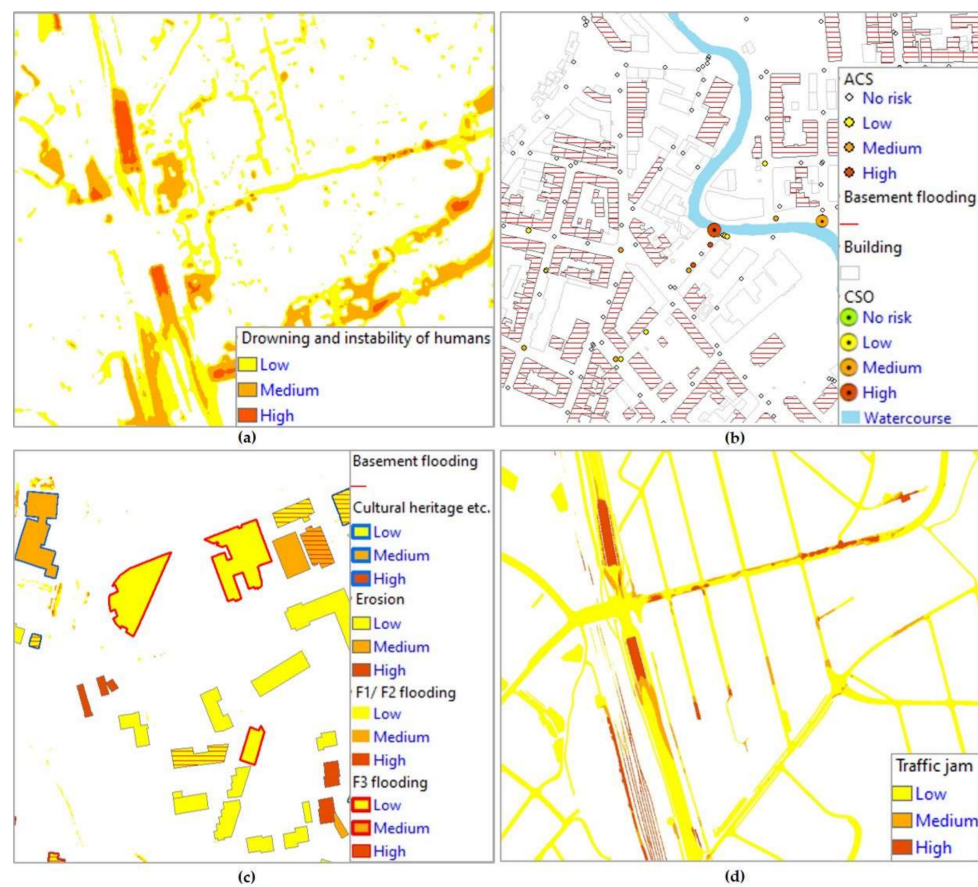


**Figure 5.** Risk of: drowning and instability of humans (a); pollution from CSO and ACS (b); building damage (c); and traffic jams (d) in the test area, Akerselva, at 200CF.

Humans can be exposed to harm in 9.5% of the total area within Akerselva at 200CF and 15.8% of the total area in the Copenhagen rain event (CPH) (Figure 6).

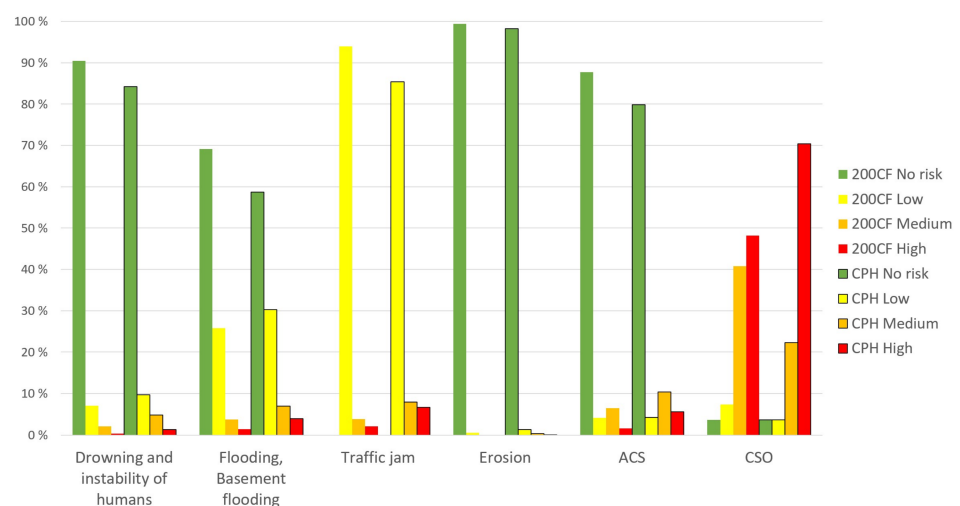


**Figure 6.** Risk distribution (no risk, low, medium, high) for different risk types for the test area (Akerselva) at 200CF and CPH in % of total area or total amount of infrastructure per risk type.

The total risk of flooding and basement flooding within Akerselva was 30.9% at 200CF. At CPH, the risk of building damage increased to 41.3% for the same area. When analysing traffic delays, no lower limit was set for the low-risk threshold. As a result, the lowest risk

was “low” for the entire road network, and no areas were assessed as “no risk”. It is thus an option to consider only medium and high risk for roads and subway and train tracks. The risk of traffic delays was medium or high for 6.0% of transport infrastructure at 200CF and 14.6% at CPH for Akerselva. The heavier precipitation event greatly increased the risk. In Akerselva, 26 of 27 CSOs were exposed to overflow discharge at both 200CF and CPH. Seven of the CSOs with medium risk at 200CF had a high risk at CPH. Total erosion risk increased from 0.6% of the total area of Akerselva at 200CF to 1.8% at CPH. 12.3% of CS manholes are exposed to ACS risk at 200CF and 20.2% at CPH.

After replacing modelling results in FME with a CPH precipitation scenario for Oslo, the corresponding visualization of consequences for different risk types was obtained for the entire city of Oslo. Visualization of risk for Oslo at CPH can be found in the supplementary materials. Results showed an exceptionally high concentration of damage risk for all risk types, except basement flooding, along closed streams. There was a risk of basement flooding from the CS throughout the city wherever there was a combined sewer system without nonreturn valves. Almost all buildings downtown were exposed to flood risk. On some stretches along open watercourses, there was a damage risk within the risk types of drowning and instability of humans, flooding, erosion, and CS overflow discharge.

### 3.2. Consequences per Risk Category

Calculation of relative consequences per risk category was performed based on Formulas (1) and (2) (Table 4).

**Table 4.** Distribution of relative consequences per subcatchment in Akerselva for each risk category (RCD1–RCD6) and total risk at 200CF. The highest value for each RCD and total risk are highlighted.

Subcatchment	Area (km <sup>2</sup> )	RCD1 Human Life and Health (%)	RCD2 Nature and Environment (%)	RCD3 Critical Infrastructure (%)	RCD4 Vulnerable Social Functions (%)	RCD5 Building Damage (%)	RCD6 Accessibility (%)	Total Risk at 200CF (%)
AKT1	0.59	43.9	28.9	13.9	42.2	55.0	57.5	40.2
AKT2	0.55	35.6	28.4	14.9	35.9	51.9	43.6	35.0
AKT3	0.70	65.5	42.5	28.6	60.5	80.8	51.8	55.0
AKT4	0.55	31.5	5.8	2.2	15.1	16.1	47.7	19.7
AKT5	0.51	36.4	44.3	2.2	9.0	13.8	51.0	26.1
AKT6	0.93	68.9	21.3	8.5	38.5	73.5	22.6	38.9
AKT7	0.60	37.9	11.4	1.8	21.2	37.8	25.3	22.6
AKT8	0.85	64.0	20.4	40.0	68.4	48.8	73.7	52.5
AKT9	0.80	54.4	18.9	28.1	39.7	68.4	56.5	44.3
AKT10	0.95	56.7	22.5	42.0	44.8	65.3	<b>89.8</b>	53.5
AKT11	1.05	71.5	20.6	<b>77.6</b>	44.5	85.0	78.5	62.9
AKT12	0.62	20.2	0.4	0.1	0.0	0.2	39.2	10.0
AKI1	0.65	51.7	<b>44.9</b>	1.5	74.0	71.4	50.5	49.0
AKI2	0.71	52.8	43.3	25.0	34.7	52.6	50.0	43.1
AKI3	1.12	43.6	22.7	62.5	28.4	27.1	88.6	45.5
AKI4	0.51	26.7	6.6	1.3	27.7	21.4	43.0	21.1
AKI5	1.17	<b>91.2</b>	36.6	32.9	<b>77.0</b>	<b>95.4</b>	45.7	<b>63.1</b>
AKI6	0.90	39.2	16.7	7.5	26.5	54.1	31.3	29.2
AKI7	0.68	30.7	6.4	18.6	17.4	31.5	26.0	21.8

Although this was an intermediate stage in calculating total risk, the information provided an increased understanding of the significance of different risk categories for total risk in different areas in the city. The Akerselva subcatchment AKI5 stood out with high relative consequences for three of the risk categories: human life and health, vulnerable social infrastructure, and building damage. AKI1, located at the mouth of the Akerselva, had the highest risk of damage to nature and the environment. AKT10, high up in the

Akerselva catchment, had the most significant risk of accessibility, and AKT11 had the highest value for distributed risk to critical infrastructure.

### 3.3. Total Risk

Calculation of total risk was performed based on Formulas (1), (2), and (3) for three different types of area distribution (Table 4). The first test for Akerselva at 200CF provided a good overview of the distribution of total risk per subcatchment (Figure 7a). The subcatchment in the middle of the Akerselva catchment, AKI5, had the highest total risk at 200CF and should be prioritized for measures if one chooses not to differentiate weighting among different risk categories.

Although only a small proportion of the area in Akerselva is exposed to erosion, erosion was included in the assessment of impact for five risk categories, and it greatly impacted the total risk. The significance of erosion was assessed by calculating the total risk with and without erosion (Figure 7b). For a scenario without erosion, the areas most exposed to damage were in the central parts of the city, where the terrain is relatively flat, and flooding was most important for the extent of damage. By including an assessment of erosion in the analysis, the distribution of total risk was changed so that areas higher up in the catchment of Akerselva, where there is steep terrain that gives high water velocity, had a higher total risk of damage than the downstream areas.

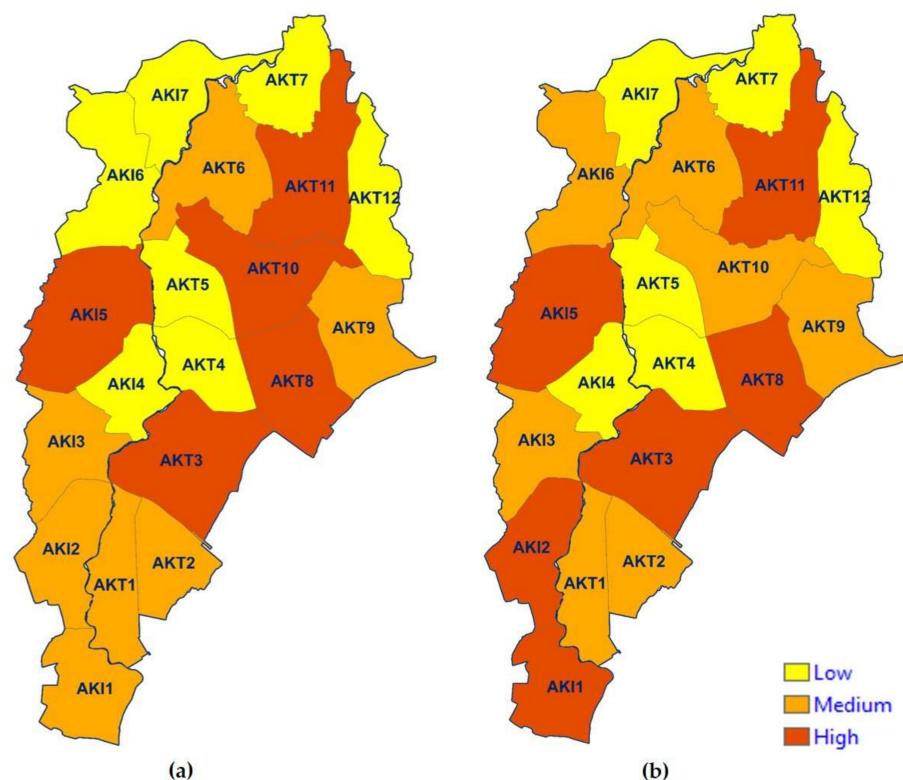


**Figure 7.** Significance of erosion for total risk. Calculated total risk including (a) vs. excluding erosion (b) for Akerselva at 200CF.

Because of the lack of division into subcatchments for the rest of the city, Oslo's initially calculated total risk at CPH was applied to the main catchments. These results could not be used to prioritize areas because of significant variations in catchment size. Therefore, the total risk for the entire city at CPH was calculated for administrative districts (see Supplementary Materials).

### 3.4. Online Visualization of Flood Risk

Results of the analysis were implemented in a visualization tool, ArcGIS online. The map in the test version of the visualization of results for Akerselva shows the risk to human life and health (Figure 8). The total number of buildings exposed to flooding was 2775 of 17,657, shown to the map's right. 74 of 189 buildings with vulnerable functions (F3) in the area were exposed to flooding. The bar graph gives an overview of risk distributed by the type of F1 and F2 facilities; e.g., approximately 440 flooded buildings were used for garages and annexes, and 200 were two-apartment houses. The dashboard also provides information on how many buildings could experience basement flooding from CS (3103 of 17,657) and how many pump stations and transformers were at risk of flooding at 200CF (10 TS/PS). At the bottom of the dashboard, the distribution of risk classes for human life and health, accessibility, and erosion are presented in bar charts. All of that information is available for the entire area and per subcatchment in this example. The desired subcatchment can be selected in the overview to the left of the map.

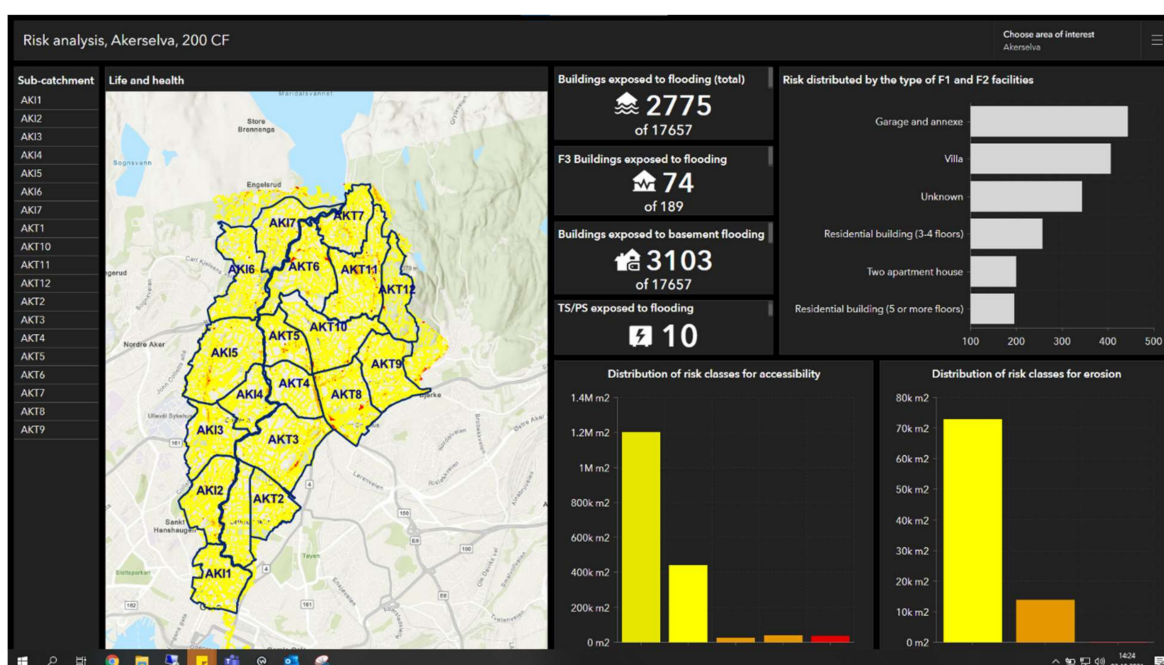


Figure 8. An example of the visualization of flood risk for Akerselva at 200CF in ArcGIS online.

## 4. Reliability

None of the data used in the study was essential for the development of the methodology or the establishment of the tool. Nevertheless, both the quality of the background data and the selected thresholds were of great importance for the outcome of the analysis.

A comparison of the relative consequence distribution for building damage with historical insurance claim data for stormwater-related building damages for the period 2008–2019 showed that approximately 2/3 of the claims coincided with the calculated damage (Figure 9).

In the insurance claims register, 5400 claims were registered due to stormwater damage in Oslo. This study showed that of 150,547 buildings in Oslo, 34,109 were exposed to damage at CPH. The common denominator for registered damage and calculated risk was that at-risk buildings were located in depressions, along historical streams, and in densely urbanized areas. However, some buildings not on the insurance damage overview would experience damage at CPH according to the study. This is because an extreme rain would affect a larger area, but Oslo has so far not experienced an event in the magnitude of CPH. There may be several reasons for why buildings on the insurance damage overview did not

receive calculated risk [9]; e.g., registrations covering a long period in which improvement measures were performed, incorrect registrations, unsure reasons for damage, different meteorological situations than CPH, or deviations in the data used as the basis for this study.

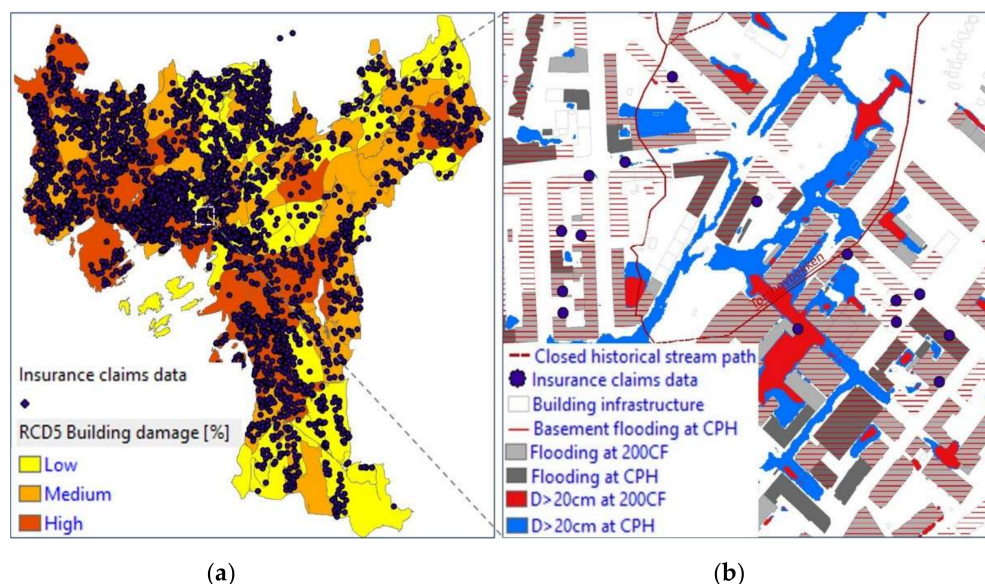


**Figure 9.** (a) Verification of registered insurance claim data vs. calculated building damage at CPH distributed on administrative districts in Oslo; (b) an example area in Oslo with coincident and noncoincident registered and calculated building damage.

A sensitivity analysis of the 1D/2D MIKE FLOOD model concluded that infiltration had considerable significance for calculation results [25]. In this study, the impact of infiltration on the outcome was assessed by running the FME model for three different sets of modelling results for Akerselva: normal infiltration, reduced infiltration by a factor of five, and increased infiltration by a factor of five. Building damage risk from flooding increased from 1111 exposed buildings in the scenario with increased infiltration to 2607 with initial infiltration and 2999 with reduced infiltration (Table 5). The effect of increased infiltration was substantial, and the risk analysis results would be more reliable if the database for infiltration for permeable areas were improved [39].

**Table 5.** Significance of infiltration for number of flooded buildings in Akerselva at 200CF.

Scenario	Number of Flooded Buildings at Different Risk Levels				Relative Numbers
	Low	Medium	High	Total	
Initial infiltration	2126	309	172	2607	100
Reduced infiltration (/5)	2404	369	226	2999	115
Increased infiltration (×5)	985	98	28	1111	43

Simulation results from the hydraulic modelling in MIKE FLOOD, which was a primary data source in this study, may deviate from reality, as the model is not calibrated. Calibration of the model against an extreme precipitation event is not possible until such event has been recorded [15]. On the other hand, it is the best database available, and when it comes to climate change, modelling is an exercise in making decisions on uncertain data.

FME codes that the FME model is set up with are reliable in principle, but it is important to consider that the coding in the FME forms a complex layout of many datasets, and there may be deviations due to human factors.

Different thresholds for drowning and instability of humans can be defined depending on age and health conditions [40]. In this study, personal injury for the weakest in society,

young children and the disabled, were considered. Several thresholds for water depth were also introduced to obtain a visually understandable result from the FME. These thresholds must be examined in more detail in further studies.

The extent of the damage from flooding in RC2, 4, and 5 was stipulated based on the perimeter of the building. There may be local variations depending on the terrain design and building construction. Information about pumping stations and transformers in RC3 may be incomplete. The height of door sills in buildings can vary, so the assumption that damage would occur at a water depth of 20 cm did not apply to all buildings.

In the study, lower thresholds were chosen for emergency routes than for other roads. Although emergency vehicles can drive through deeper water [37], they are also affected by traffic jams created by passenger vehicles. The assessment of damage risk for subway and train tracks was simplified as there is a lack of model results for the duration of flooding that could impact risk class. The lower limit for “low risk” should also be determined to identify road infrastructure that is not exposed to the risk of urban flooding.

There are reliable data on water velocities with significance for erosion, but uncertainties are associated with the created map layer showing ditch routes. Thresholds for erosion damage can also vary in different localities, depending on the condition of the ground cover. The background data can additionally be improved by excluding, for example, areas that can withstand set criteria for erosion, such as rocks and landscaped flood roads.

The uncertainties of the background data for calculating basement flooding, CSO, and ACS are related to the fact that the CS model (MIKE URBAN) and its connection to the surface need improvement and calibration. Pollutant concentrations from CS discharge should be simulated to calculate how serious the risk of pollution is. Although thresholds for basement flooding are reliable, there are uncertainties regarding the exact location of basement drains in several buildings. Thresholds for CSO and ACS risk should also be studied further.

The duration of flooding is also important for assessing the extent of damage for both nature and traffic delays. This parameter should be included in subsequent analyses.

The reliability of both background data and thresholds used in this study was considered “medium” on a scale of low–medium–high.

## 5. Discussion

Even though the total damage in Oslo could be substantial at an extreme rainfall event, there was variation in the extent of damage for different areas. Knowledge about risk variation at the local level is valuable, as it provides an opportunity to prioritize preventive measures and optimize future urban development of a climate-resistant city. The mapping and visualization of data presented in the study can contribute to a greater interdisciplinary understanding of risk issues and better communication, both of which are necessary for effective climate adaptation [9,22,29]. The risk of flooding can be investigated by studying different sets of results from the analysis.

A study of the total risk distribution for selected geographical areas is useful for prioritizing investments. The calculation and visualization of the total risk of an area should be performed for smaller, more or less equally-sized subareas. On the first test for the entire city of Oslo, the total risk was calculated per main catchment. A significant variation in catchment area gave a confusing picture of risk distribution, which was not suitable for prioritizing areas for further planning. The calculation of total risk in the test area Akerselva at 200CF was performed per subcatchment with an area of about 1 km<sup>2</sup> each. This gave a much better overview of risk distribution. As there is no complete division of subcatchments for all main catchments in the city, the total risk was instead calculated for administrative districts in Oslo.

In this study, the importance of the different risk categories was not weighted. Prioritizing of risk categories can vary among different area types in an urban environment, and this needs further interdisciplinary investigation [9]. Knowledge of risk distribution for different risk categories can be used for more targeted weighting in urban planning. The

FME model allows rapid recalculation when new information about the desired weighting is available.

Detailed information on risk for different risk types provides a good overview of damage distribution patterns on a large scale and is also useful for the development of flood risk management plans [1]. By connecting to financial thresholds on this map layer, one can obtain costs for damages [17,41].

The study results suggested that the most significant proportion of damage for most risk types lay along covered historical stream paths, especially in steep terrain. Infrastructure along small, open streams could be flooded as well. Also, historical urbanization and intervention in natural runoff pathways seemed to be among the main reasons for extensive damage from pluvial flooding at an extreme rainfall. This result is comparable to experiences from Nedre Eiker [2].

Another typical location for damage risk was near old combined sewer mains and at low points in the landscape [42], where floodwater would not find its way to the recipient, or along flat river sections. In depressions, water can penetrate buildings, cause traffic jams, spread infection, and in the worst case lead to drowning accidents. Areas with high infrastructure density in the central parts of Oslo could expect the most damage from high water depth. This result is comparable to experiences from Copenhagen, Denmark [35].

In higher-lying areas north of the city with a steep slope, the risk of erosion was considerable because of high water velocities. This result was opposite to another Norwegian study based on historical damage costs, which concluded that houses located on steep slopes seemed to be less exposed to damage [42]. The rationale for these conflicting results may be that assessing historical damage data is not necessarily representative when planning for climate change [9]. This idea would be confirmed by an example from Nedre Eiker, Norway, which was hit by 88.2 mm of rain per hour in 2012 [2]. While stormwater in the lower parts of Nedre Eiker, with downtown areas, accumulated to great depths and caused water leakage into buildings as well as traffic jams, stormwater runoff higher up in the terrain led to significant erosion damage. Large amounts of erosion masses were washed into and clogged the drainage system. Thus, the only way the floodwater could flow was on the surface. This surface flood eroded roads and building foundations. No people were injured, because the emergency service functioned effectively, and the incident occurred at night.

The results showed that it is essential to include water velocity in the analysis of flood risk in urban areas with steep and varying terrain. This was also pointed out in a study of the applicability of urban streets as temporary open floodways [42]. Water velocity data are also necessary for calculating depth-integrated velocity when assessing damage consequences for injuries and traffic jams. This information is essential for preventing the loss of human life that occurred in several floods in 2021, for instance, in Sweden [8], China [7], Germany [6], and Turkey [5].

The results of this study are, in fact, more comparable with the experience from Nedre Eiker than from Copenhagen. The results indicate that Oslo's urban flooding damage may be significantly more comprehensive than identified by the city's Municipal Risk Picture in 2017 [18], which was developed using a qualitative method based on stipulated damages from Copenhagen [35]. Despite the relatively short distance between Oslo and Copenhagen (600 km), the municipalities have significantly different topographies. The maximum elevation for Copenhagen is 99 masl. compared to 699 masl. for Oslo. Thus, the extent of damage in the Norwegian capital may be different from what the Danish capital experienced during the heavy rain in 2011.

A reliability analysis suggested that existing background data and thresholds for various risk types should be improved when better data are available. Knowing how different parameters affect the result ensures that the results are robust for decision making. Implementing a lower threshold for traffic jams can help to exclude safe transport routes from the low risk class. Knowing the number and age distribution of inhabitants living in an area at a given time and how many of them could theoretically be injured could provide

a better decision-making basis for prioritizing risk-reduction and emergency response measures [9]. Recording information about basement floor levels and nonreturn valves in the municipal database may enable a more accurate basement flooding risk calculation. Information about how many inhabitants could be affected by the malfunction of pumping stations and transformers could improve the identification of risks to critical infrastructure.

Although it is possible to obtain an overview of runoff patterns on the surface using 2D models, coupled 1D/2D models have advantages. By including watercourses in the analysis, potential constraints to floodwater diversion to the recipient are identified. Pipe networks are of great importance for the drainage of urban areas. Although the significance of pipe networks decreases during extreme precipitation [39], it is still important to assess the capacity of the largest culverts, which can be bottlenecks at ample water flows on the surface and in watercourses. Information on how the drainage pipe network behaves at different rainfall scenarios is also necessary for assessing basement flooding, CSO, and ACS risks. Because of erosion and clogging of street gullies, less runoff reaches the drainage network, reducing adverse consequences from the drainage system and leading to higher water flow and damage to the surface. The hydraulic 1D/2D model used in the study can be further developed by improving the background data. Of the improvements identified in the study, priority should be given to detailing terrain descriptions for areas exposed to damage, further developing the link between surface runoff and the pipe network, and better describing road runoff to the pipe network. Infiltration is also an essential parameter for which a better data basis should be provided. Implementing a module for calculating the pollution load from the CS will also improve the background data needed to analyse several risk categories.

## 6. Summary and Conclusions

The method and the tool for quantitative risk calculation of urban flooding developed in this study provide an opportunity to calculate the consequences for different risk categories at the given probability. The FME model combined background data from 1D/2D hydraulic modelling and GIS map layers and allowed rapid calculation of risk after changing input parameters. In the study, the tool was first developed for one of the main catchments in Oslo, Akerselva, at 200CF. After a quick switch of data sets, the calculations were run for the entire city of Oslo at CPH. The risk map for the study area was produced with the help of ArcMap and ArcGIS online.

It is essential to consider the whole city to identify the most vulnerable areas for a comprehensive prioritization of flood-protection measures. The results showed that the calculated risk of damage from urban flooding at extreme rainfall was significantly higher when several types of risk were considered and more hydraulic parameters were included in addition to water depth. Intervention in natural hydrological cycles seemed to have the most significant impact on damage, as the risk was most significant along historical stream routes. Topography is another essential aspect to consider, as the risk of erosion in steep areas significantly affected total risk. A comparison with the results of a previous risk study in Oslo [18] indicated that qualitative analysis based on other cities' flooding experiences can significantly underestimate flood risk. Using qualitative methods based on incomplete data and different geographical settings can lead to erroneous and discretionary extreme events. This may provide the wrong background data for decision making, lead to inadequate climate adaptation of urban areas, and in the worst case have dramatic consequences for inhabitants.

Although background data improvement needs were identified, the study's results were considered acceptable for the overall planning of urban flooding in Oslo. The systematic approach in this study used existing data and tools as far as possible. Therefore, the results can be considered to be the best currently available basis for decision making. Improvements mentioned in the study will gradually increase the robustness of the results. The need for enhancements should be assessed on a case-by-case basis in the continued process.

The FME model developed in this study can be implemented in other municipalities as well. The use of the tool requires access to data from hydraulic simulation for the area of interest and competence in geomatics. Although this study was based on a 1D/2D model, simulations from 2D modelling can also be used. In that case, results would be limited by which background data were used. The quality of the database is important for producing reliable results. Interdisciplinary professional competence and local knowledge about an area are essential for achieving valuable results.

The results from this study are useful both for making decisions on investment prioritization and for planning emergency preparedness and prevention measures. The analysis can be used to study the overall risk of urban flooding and assess the impact of measures at a project level. The tool can be further developed for the economic evaluation of damage under different precipitation scenarios and thus be used as part of a cost–benefit analysis to identify the socioeconomic climate adaptation level in urban areas with different characteristics.

The data in the study were limited to pluvial floods. Still, the methodology and the tool can be used to quantify the risk of urban flooding from both rivers and the sea and thereby contribute to the implementation of the Flood Directive [1] and the EU Strategy on Adaptation to Climate Change [11].

**Supplementary Materials:** The following are available online at <https://www.mdpi.com/article/10.3390/w13192771/s1>, Figure S1: Calculated total risk per main catchment in Oslo at CPH, Figure S2: Calculated total risk per administrative district in Oslo at CPH, Figure S3: Calculated relative consequence for risk category “human life and health” (RCD1) per administrative district in Oslo at CPH, Figure S4: Calculated relative consequence for risk category “nature and environment” (RCD2) per administrative district in Oslo at CPH, Figure S5: Calculated relative consequence for risk category “critical infrastructure” (RCD3) per administrative district in Oslo at CPH, Figure S6: Calculated relative consequence for risk category “vulnerable social functions” (RCD4) per administrative district in Oslo at CPH, Figure S7: Calculated relative consequence for risk category “building damage” (RCD5) per administrative district in Oslo at CPH, Figure S8: Calculated relative consequence for risk category “accessibility” (RCD6) per administrative district in Oslo at CPH, Figure S9: Distribution of risk type “drowning and instability of humans” along closed historical stream path in Oslo at CPH, Figure S10: Distribution of risk type “drowning and instability of humans” along closed historical stream path in Oslo at CPH, Figure S11: Distribution of risk type “flooding” along closed historical stream path in Oslo at CPH, Figure S12: Distribution of risk type “traffic jam” along closed historical stream path in Oslo at CPH, Figure S13: Distribution of risk type “erosion” along closed historical stream path in Oslo at CPH, Figure S14: Distribution of risk type “basement flooding” along closed historical stream path in Oslo at CPH, Figure S15. Maximum water depths with thresholds used as input in the study (CPH), Table S1: Distribution of relative risk per main catchment in Oslo for each risk category (RCD1–RCD6) and total risk at CPH.

**Author Contributions:** Conceptualization, J.K. and D.K.; methodology, J.K. and D.K.; software, T.T., J.K., and W.F.; validation, J.K., W.F., and T.T.; formal analysis, J.K. and T.T.; investigation, J.K.; data curation, J.K. and T.T.; writing—original draft preparation, J.K.; writing—review and editing, J.K., D.K., and W.F.; visualization, J.K.; project administration, J.K.; funding acquisition, J.K. All authors have read and agreed to the published version of the manuscript.

**Funding:** This research was funded by the Research Council of Norway and the Agency for Water and Wastewater, City of Oslo, as a part of public PHD 259983, “Flexible and economically sustainable stormwater management for a city growing in a changing climate”.

**Institutional Review Board Statement:** Not applicable.

**Informed Consent Statement:** Not applicable.

**Data Availability Statement:** The FME model presented in this study is available on <http://stormwaterweb.azurewebsites.net/fme/> (accessed in 1 August 2021). Access to GIS data can be applied for at [www.kartverket.no](http://www.kartverket.no) (accessed on 1 January 2021). Hydraulic model and simulations were obtained from the Agency for Water and Wastewater in the city of Oslo. Access to the data can be applied for with a request to [postmottak@vav.oslo.kommune.no](mailto:postmottak@vav.oslo.kommune.no) (accessed on 1 May 2021).

**Acknowledgments:** The authors want to extend their gratitude to the Agency for Water and Wastewater and the Agency for Planning and Building Services in the city of Oslo for giving access to the hydraulic models and map data. The authors also want to thank DHI Norway for their support with hydraulic modelling. Special thanks go to Ursula Zühlke for preparation of the background data; Kim Haukland Paus, Bent Braskerud, Oddvar Lindholm, and Jarle Tommy Bjerkholt for critical comments on the original draft preparation; and Karl Kerner at Biotext for proofreading.

**Conflicts of Interest:** The authors declare no conflict of interest. The funders had no role in the study's design, in the collection, analyses, or interpretation of data, in the writing of the manuscript, or in the decision to publish the results.

## Abbreviations

1D	One-dimensional model
200CF	200-year precipitation scenario with climate factor 1.5
2D	Two-dimensional model
ACS	Accumulation from CS manholes on the surface
CPH	Extreme rainfall in Copenhagen on 2 July 2011
CS	Combined sewer system
CSO	Combined sewer overflow
D	Water depth (m)
DEM	Digital elevation model
DV	Depth integrated water velocity (m <sup>2</sup> /s)
F1 and F2	All other buildings not covered by F3
F3	Building in category "Vulnerable social functions"
FME	Feature Manipulation Engine
GA	Geographical area of interest
masl	Metres above sea level
O	Perimeter (m)
P	Pressure in combined sewer (m)
Q	Accumulated water volume (l/s)
RC	Risk category
RCD	Relative consequence distribution
RT	Risk type
TS/PS	Electrical transformer and pumping station
V	Water velocity (m/s)

## References

1. The European Parliament and of the Council. *Directive 2007/60/EC on the Assessment and Management of Flood Risks*; PE-Cons 3618/07, Env 246 Codec 490; European Union: Brussels, Belgium, 2007; p. 8.
2. Norconsult. *Nedre Eiker—Uværet Frida August 2012 (Nedre Eiker—The storm Frida August 2012)*; Norconsult: Sandvika, Norway, 2012; p. 31.
3. Danish Emergency Management Agency. *Redegørelse Vedrørende Skybruddet I Storkøbenhavn Lørdag Den 2. Juli 2011 (Statement Regarding the Cloudburst in Greater Copenhagen on Saturday 2 July 2011)*; BRS: Birkerød, Denmark, 2012; p. 22.
4. The Local. IN PICTURES: Roads Cave in After Heavy Rain Batters Central Sweden. *The Local*. 18 August 2021. Available online: [www.thelocal.se](http://www.thelocal.se) (accessed on 18 August 2021).
5. Reuters. Heavy Floods Hit Northwest Turkey Killing 17 People. *CNN*. 13 August 2021. Available online: <https://edition.cnn.com> (accessed on 18 August 2021).
6. Kottasová, I.; Enormous Scale of Destruction is Revealed as Water Subsides after Historic Western Europe Flooding. *CNN*. 18 July 2021. Available online: <https://edition.cnn.com> (accessed on 18 August 2021).
7. Gan, N.; Yeung, J.; 'Once in a Thousand Years' Rains Devastated Central China, But There is Little Talk of Climate Change. *CNN*. 24 July 2021. Available online: <https://edition.cnn.com> (accessed on 18 August 2021).
8. Andersson, H.L.; Falkirk, J.; Mossige-Norheim, T. Kvinna Död Efter Stora Regnkaoset—Fastnade (Woman Dead After Big Rain Chaos—Stuck). *Expressen*. 26 May 2021. Available online: [www.expressen.se](http://www.expressen.se) (accessed on 18 August 2021).
9. National Academies of Sciences Engineering and Medicine. *Framing the Challenge of Urban Flooding in the United States*; National Academies Press: Washington, WA, USA, 2019; p. 89.
10. IPCC. Summary for Policymakers. In *Climate Change 2021: The Physical Science Basis*; Cambridge University Press: Cambridge, UK, 2021; p. 41.

11. European Commission. *Forging a Climate-Resilient Europe—The New EU Strategy on Adaptation to Climate Change*; European Commission: Brussels, Belgium, 2021; p. 22.
12. Swedish Civil Contingencies Agency. *Vägledning för Riskhanteringsplaner (Guidance for Risk Management Plans)*; MSB: Karlstad, Sweden, 2020.
13. Peereboom, I.O.; Waagø, O.S.; Myhre, M. *Preliminary Flood Risk Assessment in Norway*; Norwegian Water Resources and Energy Directorate: Oslo, Norway, 2011; p. 46.
14. Norwegian Directorate for Civil Protection. *Risikoanalyse Av Regnflom I By (Risk Analysis of Urban Flooding)*; DSB: Tønsberg, Norway, 2016; p. 72.
15. Swedish Civil Contingencies Agency. *Vägledning För Skyfallskartering. Tips För Genomförande Och Exempel På Användning (Guidance for Rainfall Mapping. Tips for Implementation and Examples of Use)*; MSB: Karlstad, Sweden, 2017; p. 72.
16. Willows, R.; Reynard, N.; Meadowcroft, I.; Connell, R. Climate adaptation: Risk, uncertainty and decision-making. Part 2. In *Climate Impacts Programme, 41–87*; (UNSPECIFIED): Oxford, UK, 2003; p. 50.
17. Scorzini, A.R.; Leopardi, M. River basin planning: From qualitative to quantitative flood risk assessment: The case of Abruzzo Region (central Italy). *Nat. Hazards* **2017**, *88*, 71–93. [\[CrossRef\]](#)
18. Andersson-Sköld, Y.; Davidsson, G. *Riskhänsyn Vid Hantering Av Översvänningsrisker (Risk Considerations When Managing Flood Risks)*; COWI: Gothenburg, Sweden, 2016; p. 85.
19. Nordeidet, B.; Hansen, C.B. *Ekstremnedbør. Oslo. Skadeomfang og Kostnader (Extreme rainfall. Oslo. Extent of Damage and Costs)*; Rambøll: Oslo, Norway, 2019; p. 65.
20. World Bank. *Learning from Japan's Experience in Integrated Urban Flood Risk Management: A Series of Knowledge Notes. Knowledge Note 1: Assessing and Communicating Urban Flood Risk*; World Bank: Washington, DC, USA, 2019; p. 40.
21. City of Oslo. *Kommunalt risikobilde 2017. Kortversjon (Municipal risk picture 2017. Short version)*; Emergency Planning Agency: Oslo, Norway, 2017; p. 36.
22. Norwegian Directorate for Civil Protection. *Analyses of Crisis Scenarios 2019*; DSB: Skien, Norway, 2019; p. 228.
23. Mårtensson, E.; Gustafsson, L.-G. *Kartläggning av Skyfalls Påverkan på Samhällsviktig Verksamhet (Mapping of the Extreme Rain Impact on Critical Infrastructure)*; DHI: Malmö, Sweden, 2014; p. 64.
24. Mackay, C.; Suter, S.; Albert, N.; Morton, S.; Yamagata, K. Large scale flexible mesh 2D modelling of the Lower Namoi Valley. In *Floodplain Management Association National Conference*; Floodplain Management Australia: Brisbane, QLD, Australia, 2015.
25. Liang, Q.; Zhang, H.; Liu, Z. A coupled hydrological and hydrodynamic model for flood simulation. *Hydrol. Res.* **2019**, *50*, 589–606.
26. Zhang, W.; Zhang, X.; Liu, Y.; Tang, W.; Xu, J.; Fu, Z. Assessment of Flood Inundation by Coupled 1D/2D Hydrodynamic Modeling: A Case Study in Mountainous Watersheds along the Coast of Southeast China. *Water* **2020**, *12*, 822. [\[CrossRef\]](#)
27. Zhao, G.; Balstrøm, T.; Mark, O.; Jensen, M.B. Multi-Scale Target-Specified Sub-Model Approach for Fast Large-Scale High-Resolution 2D Urban Flood Modelling. *Water* **2021**, *13*, 259. [\[CrossRef\]](#)
28. Almestad, C. *Flommodell Oslo kommune. Modelldokumentasjon MIKE FLOOD (Flood Model Oslo Municipality. Model Documentation MIKE FLOOD)*; Agency for Water and Wastewater Services: Oslo, Norway, 2021.
29. FME. *Feature Manipulation Engine*; SAFE SOFTWARE: Surrey, BC, Canada, 2021.
30. ArcMap ArcGIS Online. *Products*; ESRI: California, USA, 2021.
31. MET. *Nedbørsstatistikk (Precipitation Statistics)*; The Norwegian Meteorological Institute: Oslo, Norway, 2019.
32. City of Oslo. *Hovedplan Vann Og Avløp 2020–2040 (Master Plan for Water and Wastewater 2020–2040)*; Agency for Water and Wastewater Services: Oslo, Norway, 2020; p. 55.
33. MIKE Powered by DHI, MIKE FLOOD, MIKE URBAN, MIKE21, MIKE HYDRO River, MIKE View, MIKE Zero, in MIKE Powered by DHI. 2020, DHI, Hørsholm, Denmark.
34. Dyrredal, A.V.; Førland, E.J. *Klimapåslag for Korttidsnedbør. Anbefalte Verdier For Norge (Climate Surcharge for Short-Term Precipitation. Recommended Values for Norway)*; NCCS Report; Norsk Klimaservicesenter: Stavanger, Norway, 2019; p. 25.
35. Norwegian Building Authority. *Byggeteknisk Forskrift (TEK17). Kapittel 7 Sikkerhet Mot Naturpåkjenninger (Building Regulations (TEK17). Chapter 7 Safety Against Natural Stresses)*; Norwegian Building Authority: Norway, Oslo, 2017.
36. Lindholm, O.; Buhler, L.; Bjerkholt, J. Hva hvis monsterregnet fra København 2. juli 2011 hadde falt i Norge? (What if the monster rain from Copenhagen on 2 July 2011 had fallen in Norway?). *VANN* **2013**, *3*, 10.
37. City of Oslo. *Sanitærreglement for Oslo. Tilknytnings- Og Abonementsbetingelser for Sanitæranlegg (Sanitary Regulations for Oslo. Connection and Subscription Conditions for Sanitary Facilities)*; Agency for Water and Wastewater Services: Oslo, Norway, 1982; p. 15.
38. Schmitt, T.G.; Scheid, C. Evaluation and communication of pluvial flood risks in urban areas. *WIRES Water* **2019**, *7*, e1401. [\[CrossRef\]](#)
39. Persson, J.; Karlsson, A.; Jansson, K.; Gustavsson, L.-G. *Skyfallsmodellering För GBG. Avrinningsanalyz Med 2-Dimensionell Hydraulisk Modell Som Beskriver Vattenansamling Och Avrinningsvägar I Stora Delar Av Göteborgs Kommun Vid 100- Och 500-Årsregn (Rainfall Modelling for GBG. Drainage Analysis with A 2-Dimensional Hydraulic Model that Describes Water Accumulation and Drainage Routes in Large Parts of Gothenburg Municipality During 100- and 500-Year Rains)*; Sweco, DHI: Gothenburg, Sweden, 2015; p. 67.
40. Martínez-Gomariz, E.; Gómez, M.; Russo, B. Experimental Study of the Stability of Pedestrians Exposed to Urban Pluvial Flooding. *Nat. Hazards* **2016**, *82*, 1259–1278. [\[CrossRef\]](#)

- 
41. Torgersen, G.; Rød, J.K.; Kvaal, K.; Bjerkholt, J.T.; Lindholm, O.G. Evaluating Flood Exposure for Properties in Urban Areas Using a Multivariate Modelling Technique. *Water* **2017**, *9*, 318. [[CrossRef](#)]
  42. Skrede, T.I.; Muthanna, T.M.; Alfredesen, K. Applicability of urban streets as temporary open floodways. *Hydrol. Res.* **2020**, *51*, 621–634. [[CrossRef](#)]